OPTICAL REVIEW Vol. 11, No. 6 (2004) 1–5

Near Field Observation of a Refractive Index Grating and a Topographical Grating by an Optically Trapped Gold Particle

Hiroo UKITA*, Hirotaka UEMI† and Atsuhiro HIRATA

Faculty of Science and Engineering, Ritsumeikan University, 1-1-1, Nojihigashi, Kusatsu-shi, Shiga 525, Japan

(Received April 21, 2004; Accepted September 3, 2004)

We observed the near field for a refractive index grating fabricated on a planar light waveguide circuit (PLC) by scanning an optically-trapped 100 nm diameter gold particle. We demonstrate that stable trapping and scanning occur with a Gaussian laser beam at the scan velocity of 1.6 μm/s and Nd:YAG laser power of 25 mW. The scattered Ar^+ laser light from the gold particle is strong at high refractive indexes of the grating with periods of 1.06 μm and 0.53 μm, both by s and p polarized illumination. In addition, we observed the surface profile of the optical disk tracking groove with and without the gold particle.

Key words: near field, optical tweezers, refractive index grating, planar light waveguide circuit, PLC, gold particle, optical trapping, polarization, groove

1. Introduction

It is well known that surface plasmon (SP) existing on metal surfaces and metal/dielectric interfaces causes strong field enhancement at the interface.[1–3] According to the theoretical analysis, surface refractive index distribution mapping with high contrast is predicted to be possible.[4] These are the principles of operation in scattering-type scanning near-field optical microscopy (SNOM).[5,6]

A metal particle probe is considered to have the advantages of: (1) high experimental reproducibility from particles being made to the same shape and size; (2) does not require control from a distance, and (3) not only to have the ability to obtain an image, but also the spectroscopic data of the sample. The scattering efficiency of a silver particle is higher than that of a gold particle, but the latter is more chemically stable.[7] Therefore, a gold particle is frequently used as a SNOM probe. T. Sugiura *et al.*, observed a dip on a cover glass and a gold colloidal particle adhering to the cover glass.[5] However, these images were thought to have an artifact problem due to the vertical displacement of the gold probe.[8]

On the other hand, we demonstrated observation of a refractive index grating on a flat surface, which was made on a planar light waveguide circuit (PLC), by scanning an optically-trapped 100 nm diameter gold particle.[9] The scattered Ar^+ laser light from the gold particle was strong due to the high refractive index of the grating with periods of 1.06 μm and 0.53 μm, both by s and p polarized illumination. We also observed the surface profile of an optical disk tracking groove with and without the gold particle and compared the results to discuss the artificial effect due to the vertical displacement of the particle caused by the surface topology.

2. Experimental Setup

Figure 1(a) shows an experimental setup to trap a gold particle with an upward-directed Nd:YAG laser beam ($\lambda = 1.06\,\mu m$) and to scan it on the sample surface two-dimensionally by using an XY stage. The upward-directed beam has a significantly higher trapping efficiency than the downward one.[10] The gold particle at the focal point of the NA = 1.3 immersion oil objective lens is in the medium of a coverslip chamber and is pushed onto the sample

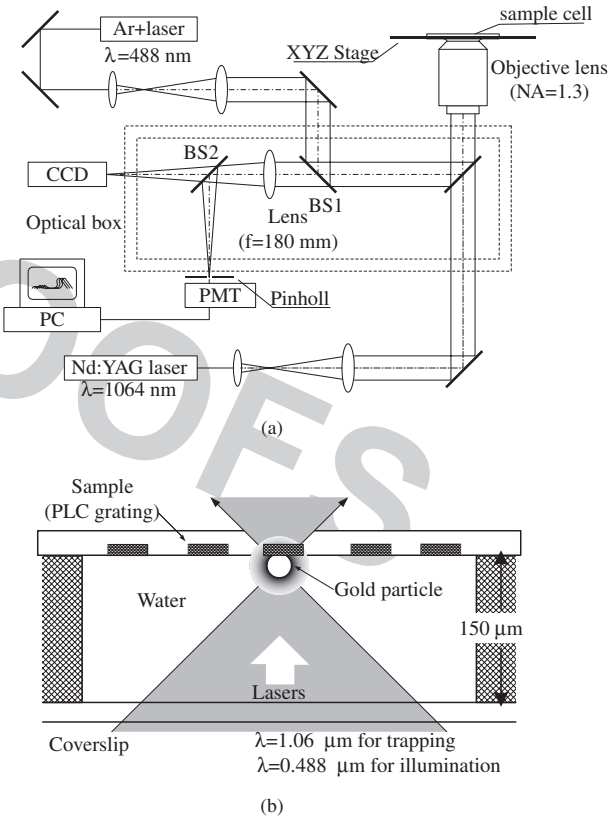

Fig. 1. (a) Experimental setup of the SNOM using an optically-trapped gold particle. A Nd:YAG laser is used to trap, and an Ar^+ laser is used to illuminate the gold particle. All the optical elements except the mirrors to guide the two lasers are installed inside the optical box for easy operation. (b) Enlarged view of the sample chamber.

*E-mail address: ukita@se.ritsumei.ac.jp
†Currently with Matsushita Denko Corporation, Kadoma, Osaka 571, Japan.

surface, as described later, and scanned as shown in Fig. 1(b).

An Ar^+ laser ($\lambda = 488$ nm) is focused through the same objective to illuminate the particle. The scattered light from the gold particle is collected through the objective and imaged on the pinhole (5 μm in diameter) in front of a photo multiplier tube (PMT). The scattered light variation due to the interaction between the gold particle and the sample surface is recorded through a personal computer (PC). A CCD camera observes the operation of the gold particle in the medium. All the optical elements, except the mirrors to guide the Nd:YAG laser and Ar^+ laser, are installed inside the optical box for easy operation.

3. Optical Trapping Characteristics of a Gold Particle

3.1 Trapping principle

A metallic Rayleigh particle (much smaller than the wavelength) can be optically trapped at the focal point by the gradient force of a strongly focused laser beam.[11] The gradient force F_{grad} for the Rayleigh particle is given by

$$F_{\mathrm{T}} = \frac{1}{4} n_{\mathrm{m}} \alpha \,\mathrm{grad}(|E|^2), \tag{1}$$

where α is the polarizability of the gold particle and E is the electric field. The polarizabiliy is given as

$$\alpha = 4\pi\varepsilon\varepsilon_0 \frac{m^2 - 1}{m^2 + 2} r^3, \tag{2}$$

where m is the relative refractive index of the particle to the medium (n/n_{m}), r is the radius of the particle and ε_0 is the dielectric constant in vacuum.

The F_{grad} in the transverse direction and in the axial direction were calculated for the gold particle refractive index $n = 0.272 + \mathrm{i}7.07$, the gold particle diameter $2r = 100$ nm, the medium refractive index $n_{\mathrm{m}} = 1.33$, the objective lens NA = 1.3, and the Gaussian laser power is 20 mW. We found that the gradient force along the transverse direction was eight times greater than that along the axial direction. This result shows that the trapping particle is more stable along the transverse direction but unstable along the optical axis which leads to upward-directed beam to trap the particle and to push it onto the sample surface.

3.2 Dependence on scanning velocity

The theoretical lateral trapping power P_{lat} can be expressed in Eq. (3) by considering the maximum trapping efficiency $Q_{\max}$,

$$P_{\mathrm{lat}} = 3\pi\eta dvc(1 + 9d(1/T - 1/(H - T))/32)/n_{\mathrm{m}}Q_{\max}, \tag{3}$$

where η and n_{m} are the viscosity and the index of refraction of the suspending medium, respectively; c is the speed of light, and H is the height of the specimen chamber (150 μm).[12] $Q_{\max}$ is found from the maximum gradient force at $1.49/(2\pi/\lambda)\mathrm{NA} = 193$ nm along the transverse direction.[11]

Although the calculated result is based on an aberration-free optical system, the actual trapping characteristics are affected by the color aberration of the objective lens (for near infrared $\lambda = 1.06$ μm) and the spherical aberration due to the refractive index difference between the immersion oil (1.52) and the medium (1.33).

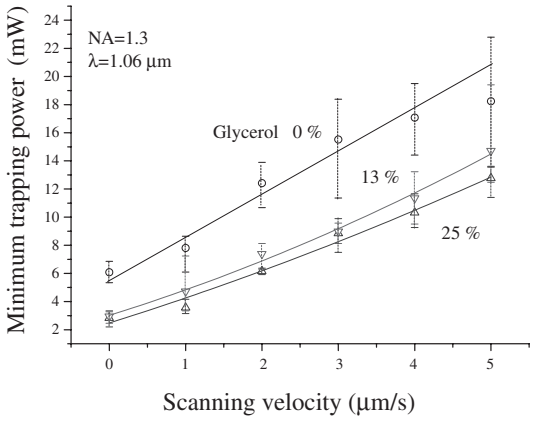

Fig. 2. Dependence of the minimum axial trapping power on the scanning speed of an optically-trapped gold particle.

Figure 2 shows the dependence of the minimum trapping power $P_{\min}$ on the scanning velocity of an optically-trapped gold particle for different viscosities which were controlled by altering the glycerol density. The $P_{\min}$ was measured as the minimum power needed to trap the bead moving at the velocity of v in water. The minimum trapping power increases as the scanning velocity increases, but decreases as the viscosity increases. The addition of the glycerol is effective in decreasing the Brownian motion by increasing the viscosity.

4. Observation of a PLC Refractive Index Grating

The sample for the trapped-particle probe is a refractive index grating fabricated by UV exposure through a phase mask under the conditions outlined in Table 1.[9] The grating is formed in a clad layer (30-μm thick) on a planar light waveguide circuit (PLC) as shown in Fig. 3, where the top view of the grating is shown by optical microscopy. The grating period of 1.06 μm (zeroth order) is clearly seen but the grating period of 0.53 μm (first order) is only partially visible. The relative refractive index difference between the gratings in the clad layer is estimated to be 0.001 to 0.002 where the clad layer index is 1.45.

We observed the scattered Ar^+ laser light ($P = 0.13$ mW) by the 100 nm gold particle optically-trapped by an Nd:YAG

Table 1. Conditions to fabricate a refractive index grating in PLC.

Core (SiO_2+GeO_2) index	1.46
Clad (SiO_2) index	1.45
Refractive index difference	0.001 ~ 0.002 (Estimate)
Phase mask method	Source: ArF laser ($\lambda = 193$ nm)
	Phase mask pitch: 1.06 μm
	Energy density per pulse: 1.0 J/cm^2/pulse
	Pulse repetition rate: 50 Hz
	Grating pitch (Zero order): 1.06 μm

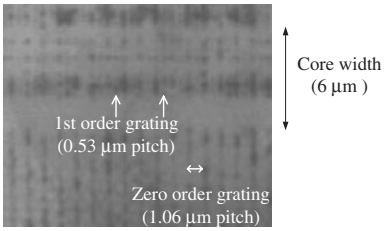

Fig. 3. Photograph of a refractive index grating fabricated on a planar light waveguide circuit.

($P = 25$ mW) laser, which was scanned over the refractive index grating at the PLC surface. The scanning velocity and pitch were 1.6 μm/s and 50 nm, respectively. Observation time for the square 5 μm × 5 μm area was five minutes.

Figure 4 shows the SNOM images of the refractive index grating produced by a gold particle probe with p-polarized illumination (electric field is perpendicular to the gratings as shown). Figure 4(a) shows the scattered light intensity, while Fig. 4(b) shows the gray scale image. Figure 5 shows Fig. 5(a) the scattered light intensity and Fig. 5(b) the gray scale image with s-polarized illumination (electric field is parallel to the gratings as shown). We can clearly recognize the grating pitch of 1.06 μm in all the images.

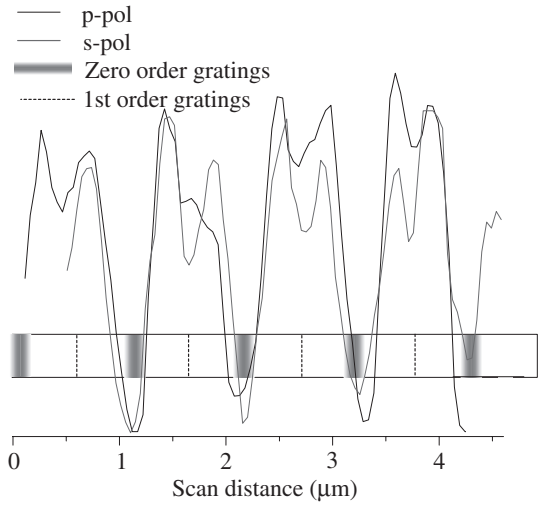

Fig. 6. Relationship between scattered light intensity and refractive index grating distribution.

Figure 6 shows the relationship between scattered light intensity and the refractive index grating distribution. The scattered lights are averaged for ten data lines. The scattered averaged light corresponds to the grating distribution of the

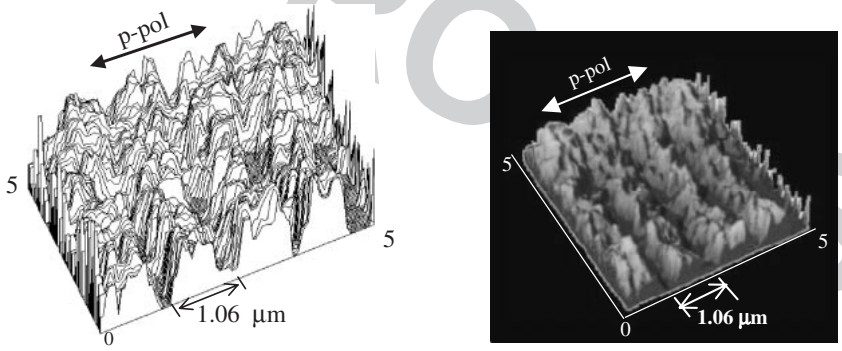

(a) (b)

Fig. 4. SNOM images of the refractive index grating by a gold particle probe with p-pol illumination, (a) Scattered light intensity, (b) Gray scale image.

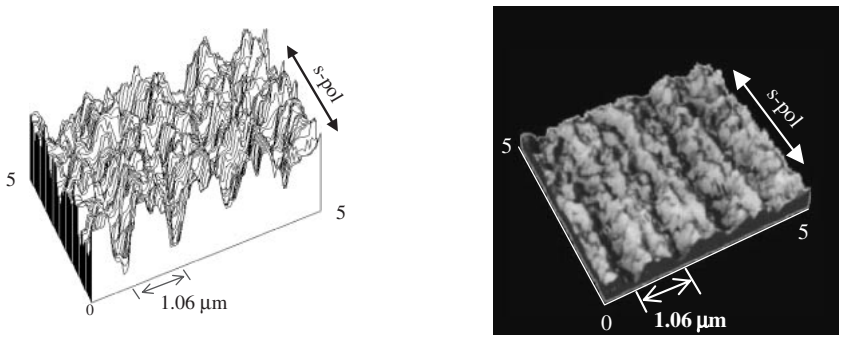

(a) (b)

Fig. 5. SNOM images of the refractive index grating by a gold particle probe with s-pol illumination, (a) Scattered light intensity, (b) Gray scale image.

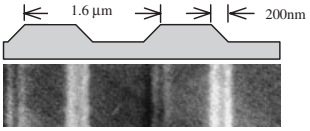

Fig. 7. SEM photograph of an optical disk groove and its profile.

periods of 1.06 and 0.53 μm for both p-pol and s-pol illumination. The higher order grating of 0.53 μm can also be seen by the 100 nm gold particle. By collecting the scattered light under a scanning gold particle that induces a local electric field, we have resolved two individual refractive index periods on the sample surface. We confirm that the optical near field is effective for observing the sample surface beyond the diffraction limit of optical microscopy.[7,13,14)]

Next, we investigated the possibility of profiling the topography of the sample surface. Figure 7 shows a sectional view of the optical disk tracking groove, which is observed via scanning electron microscopy (SEM). The period is 1.6 μm, 0.1 μm deep, and the groove edge width is 200 nm.

Figure 8 shows the SNOM topography profile by a gold particle probe under p-pol illumination with the addition of glycerol (13%); (a) is a scattered light intensity image, while (b) is a gray scale image. We can clearly see the groove pitch of 1.6 μm, both with and without the gold probe.

Figure 9 shows the relationship between the averaged scattered light intensity and the groove profile. The scattered light from the gold particle (thin solid line) is strong at the groove edge and has split peaks for p-pol illumination. The scattered light without gold particle (dashed line) is weak and has a single peak at the groove edge. The difference between the two (bold solid line) seems to correspond to the surface topology because the effect of the laser light reflection is removed.

5. Conclusions

An experimental setup to trap a 100 nm gold particle with an upward-directed Nd:YAG laser beam ($\lambda = 1.06\,\mu$m) and to scan over the sample surface was constructed. We observed the refractive index grating and the topographical grating by near field optical microscopy.

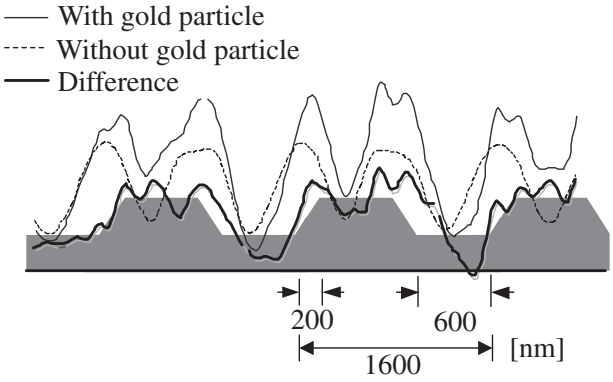

Fig. 9. Relationship between scattered light intensity and disk groove profile with and without a gold particle.

First, we observed the refractive index grating which contains no artifact caused by surface topology. The pitches were 0.53 μm and 1.06 μm, fabricated by UV exposure through a phase mask on a planar light waveguide circuit (PLC). The amplitude for the refractive index modulation of the clad layer (index 1.45) is estimated to be between 0.001 to 0.002. The scanning velocity and pitch were 1.6 μm/s and 50 nm, respectively. Five minutes were taken to observe the square 5 μm × 5 μm sample area. A comparison between the scattered light intensity and the refractive index grating distribution led to each corresponding with both p-pol and s-pol illumination.

Second, an observation under p-polarization was also made of the topographical optical disk tracking groove. The scattered light from the gold particle was strong at the groove edge and had split peaks, whereas the scattered light without the particle had no split peaks. The difference between the two seems to correspond to the surface topology.

From the result above, we confirm that an optically trapped gold particle is effective in observing both physical and topological properties of a sample.

Acknowledgements

The authors would like to thank Drs Toru Maruno and Yoshinori Hibino of NTT Photonics Laboratories for fabrication of the PLC grating.

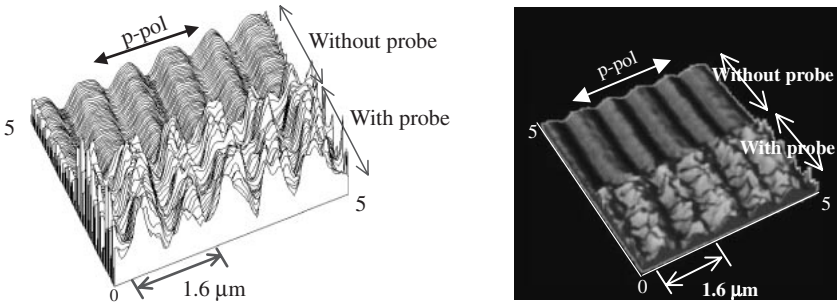

Fig. 8. SNOM topography of the optical disk tracking groove by a gold particle probe with p-pol illumination, (a) Scattered light intensity, (b) Gray scale image.

References

1) H. Raether: *Surface Plasmons*, ed. G. H. Föhler (Springer-Verlag, Berlin, 1988) Springer Tracts in Modern Physics vol. 3.
2) L. Novotny, R. X. Bian and X. S. Xie: Phys. Rev. Lett **79** (1997) 645.
3) H. Furukawa and S. Kawata: Opt. Com. **148** (1998) 221.
4) T. Okamoto and I. Yamaguchi: Opt. Rev. **6** (1999) 211.
5) T. Sugiura, T. Okada, Y. Inoue, O. Nakamura and S. Kawata: Opt. Let. **22** (1997) 1663.
6) M. Gu and P. C. Ke: Opt. Lett. **24** (1999) 76.
7) H. Tamaru, H. Kuwata, H. T. Miyazaki and K. Miyano: Appl. Phys. Lett. **80** (2002) 1826.
8) B. Hecht, H. Bielefeldt, Y. Inoue and D. W. Pohl: J. Appl. Phys. **81** (1997) 2492.
9) K. O. Hill, B. Malo, F. Bilodeau, D. C. Johnson and J. Albert: Appl. Phys. Lett. **62** (1993) 1035.
10) H. Ukita and T. Saitoh: *IEEE Lasers and Electro-Optics Society 1999 Annual Meeting*, ed. Chris Harder (San Francisco, 1999) Vol. 1, p. 169.
11) T. Sugiura: *Near-field optics and surface plasmon polaritons*, ed. S. Kawata (Springer, Tokyo, 2001) p. 143.
12) H. Felgner, O. Muller and M. Schliwa: Appl. Opt. **34** (1995) 977.
13) J. R. Krenn, A. Dereux, J. C. Weeber, E. Bourillot, Y. Lacrout and J. P. Goudonnet: Phys. Rev. Lett. **82** (1999) 2590.
14) Y. C. Martin, H. F. Hamann and H. K. Wickramasinghe: J. Appl. Phys. **89** (2001) 5774.